Performance investigation of a novel Franchot Engine design

Performance investigation of a novel Franchot Engine design

Jafar Daoud, Daniel Friedrich*

Institute for Energy Systems, School of Engineering, University of Edinburgh, EH9 3DW (Scotland)

**Corresponding author Email: d.friedrich@ed.ac.uk*

Abstract: *The double-acting Franchot engine is inferior to the double-acting Siemens engine under configurations limited by the Siemens engine. In this contribution, the performance of a novel Franchot engine design without the Siemens engine limitations is investigated with a new mathematical definition of the regenerator end temperatures and the initial statement is challenged. The main advantages of the Franchot engine compared to the Siemens engine are the free control of the phase angle and the thermal separation of the cylinders. Here the performance of a cylinder heated/cooled air filled Franchot engine is investigated at medium temperature under variations of engine speed, phase angle, geometry, dead volume and gas density. A second order thermodynamic model with non-constant, polytropic heat transfer is developed and implemented in Matlab/Simulink for this investigation. The non-constant heat transfer is crucial to accurately model the behaviour of the direct cylinder heating and cooling. The results show that the phase angle and air charge density have the largest effect on the engine performance. An increase of the phase angle from 90° to 150° at a speed of 1000RPM led to an increased output power of 58W compared to a maximum power less than 20W for a phase angle of 90°. The efficiency at a phase angle of 150° is approximately 25% which is a bit lower than the ideal Curzon and Ahlborn efficiency of 29.3%. This discrepancy can be explained by the non-constant, polytropic heat transfer. In addition to the increase in engine power, the operation at higher phase angles reduces the pressure difference across the power piston by a factor larger than 4 which leads to a significant reduction in gas leakage across the power pistons. This shows that at higher phase angles the two main disadvantages compared to the Siemens engine are at least reduced and arguably completely removed. Thus the Franchot engine has the potential to be superior to the Siemens engine if freed from the operational restrictions of the Siemens engine.*

Keywords: *Franchot engine; double acting Stirling engine; instantaneous polytropic heat transfer; non-tubular, direct heated/cooled*

Nomenclature

A_x *Total cylinder wall area [m²]*

c_v *Gas heat capacity at constant volume [J/kg.K]*

c_p *Gas heat capacity at constant pressure [J/kg.K]*

D_x *Cylinder bore in each compartment [m]*

f *Engine frequency [Hz]*

h *In cylinder heat transfer coefficient [w/m².K]*

L_e *Total expansion cylinder length [m]*

L_c *Total compression cylinder length [m]*

M *Total working gas mass [kg]*

m_x *Gas mass in compartment x [kg]*

n *Engine speed [RPM]*

Nu *Nusselt number*

p *Instantaneous gas pressure [N/m²]*

P *Average mechanical power [W]*

P_{ins} *Instantaneous mechanical power [W]*

Q_x *Heat exchanger thermal energy [J]*

rc *Compression space clearance [m]*

re *Expansion space clearance [m]*

R *Ideal gas constant [J/kg.K]*

Re *Reynolds number*

T_x *Instantaneous temperature [K]*

v_x *Volume of compartment x [m³]*

w *Cycle work [J]*

Greek letters

γ *Heat capacity ratio*

ρ *Charge gas density [kg/m³]*

θ *Out of phase angle [deg]*

Subscripts

c Compression space

e Expansion space

h *Hot cylinder*

k *Cold cylinder*

r *Regenerator*

rh *Regenerator hot side*

rk Regenerator cold side

x Represent specific compartment

1. Introduction

The Stirling engine is an external combustion engine which was patented by Robert Stirling in 1816 [1]. Stirling engines are characterised by their simplicity, safe and quiet operation, efficiency and ability to run on any thermal source. This makes them particularly suited for the transformation of medium temperature solar energy to mechanical or electrical energy which opens the potential for widespread application in regions with strong solar irradiance.

Stirling engines running on high temperature differences have a large range of applications and can achieve high power densities and efficiencies [2]. However, so far Stirling engines haven't been widely deployed due to a number of remaining challenges: working fluid leakage; large volume and weight; low compression ratio due to the heat exchangers [3]; complexity of the materials used to manufacture the engine, heat exchangers and solar thermal collectors; and total system cost [2][4]. On the other hand, medium temperature Stirling engines (up to 600K) can use simpler and cheaper technologies and materials which reduce the severity of the above mentioned challenges. In addition, the low temperature heat can be provided through solar line concentrators [5][2] or waste heat from industrial sources. Low temperature differential (LTD) Stirling engines are characterised by large compression ratios, large displacer diameter, short displacer length, small displacer stroke and low operating speed [6]. However, the advantages of LTD Stirling engines are balanced by lower efficiency and power density compared to high temperature difference Stirling engines.

Stirling engines can be classified according to their mode of operation into: single acting, in which gas is in contact with only one piston face and double acting engines, which were developed by Babcock in 1885, in which the working gas is in contact with both sides of the piston [1]. Figure 1 shows the Franchot and Siemens double acting, multi-cylinder engines in which each expansion compartment is connected to a compression compartment through heat exchangers, namely: heater, regenerator and cooler. These engines compromise many features which make them preferable over single acting engines: half the number of reciprocating parts, which results in simpler kinematics [7], absence of the displacer, no need for the bounce space or pressurised crankcase, compactness and high power density.

The conventional Stirling engine uses unheated and uncooled cylinders and, instead, has tubular heaters and coolers (see Figure 1). Those heat exchangers add to the dead volume of the regenerator, the clearance volumes, and the connecting lines. The dead volume is also referred to as the un-swept volume which ideally should be zero [1]. However, in practice dead volumes make up over 50% of the total engine volume [3]. Directly heating the expansion cylinder and cooling the compression cylinder instead of using the tubular heater and cooler reduces the total dead volume and pressure drop in the engine. However, in this configuration the heat transfer is challenging and it is necessary to use an isothermalizer or other methods to improve the gas to wall heat transfer [8].

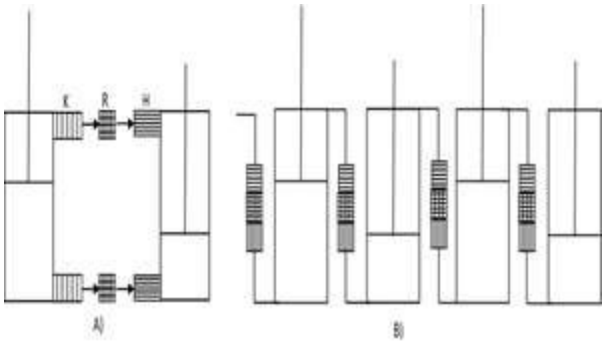

Figure 1: Double acting Stirling engines. A) Franchot engine and B) Siemens engine. The pistons are connected through the cooler (K), regenerator (R) and heater (H).

The Franchot engine which is shown in Figure 1A was invented in the 19th century and is attributed to Charles Louis Franchot [9]. In contrast to the related Siemens engine (Figure 1B), only two pistons are required for an engine, the phase angle can be freely controlled and each piston is either hot or cold which eliminate the shuttle and conduction losses [10]. However, it has received only limited attention due to piston sealing problems in the hot cylinder. Keeping the seal at an acceptable temperature level in the hot cylinder is less severe for medium temperatures and can be neglected completely by using a clearance seal [11]. Low friction PTFE seals can be used at temperatures up to 300^{o} C [2]. Graphite seals can be used at even higher temperatures but are limited to 400^{o} for air to prevent carbonising. Thus the Franchot engine can be a good alternative at these temperatures.

A recent study by Hoegel [11] compared both the Siemens and the Franchot engines. He found that the Siemens engine is superior to the Franchot engine at the same operational conditions. This is mainly due to gas leakage through the power pistons due to a higher pressure difference in the Franchot engine at a 90^{o} phase angle. He showed that the 30% difference in the pressure amplitude at 90^{o} phase angle was responsible for increasing the losses from 0.1% (in the Siemens engine) to 3.9% (in the Franchot engine). However, the pressure difference can be reduced by increasing the phase angle and dead volume. In addition, increasing the phase angle leads to an increase in the heat transfer and thus the conventional choice of the 90^{o} phase angle is mainly due to mechanical design reasons [12].

In fact, many researchers [12][13][14] showed that it is important to tune the phase angle to achieve the optimal performance of a Stirling engine. Martaj and Rochelle [15] studied the Franchot engine with a common recuperator-regenerator and showed that an increase in efficiency of 18% was obtained for a phase angle of 120^{o} in comparison to 110^{o}. Hoegel [11] showed that the maximum power occurs around 150^{0} and 160^{0} for hydrogen and helium charged engines, respectively. For nitrogen the engine gave negative power at 150^{o} and he had to increase the heat transfer to achieve positive power. This shows that the optimal phase angle critically depends on the heat transfer rate. The difference in optimal phase angle between hydrogen and helium is due to the different thermal conductivities. While these findings indicate the importance of tuning the phase angle, so far no rigorous study investigating the effect of the phase angle on the efficiency and power of the Franchot engine has been performed.

The power and efficiency of Stirling engines can be mathematically predicted using thermodynamic models which are classified into: zero, first, second and third order models. Zero order models are based on experimentally derived numbers, such as the Beale number, which link the power output to easily measured quantities such as engine speed and average pressure [16]. However, these models cannot be used to predict the performance change due to changes in the configuration such as different strokes, bores, driving mechanism and phase angle. The first order or analytical model uses algebraic equations to describe the engine performance. In 1871 Schmidt was able to describe analytically the isothermal expansion and compression of a closed cycle [17]. His ideal model approaches Carnot efficiency and can approximately predict the performance of a

Stirling engine [17]. In 1975 Curzon and Ahlborn [18] corrected the Carnot efficiency at the maximum output power under the assumption of isothermal expansion and compression processes based on finite time thermodynamics at which the heat transfer is finite. The second and third order models use differential equations in time and in time and space, respectively. These models have been studied extensively since Finkelstein's first second order adiabatic model in 1960 [19]. Among the mathematical models, the second order and third order models are the most accurate [20]. While the first, second and third order models can all be used to analyse the isothermal, adiabatic and semi adiabatic operation of Stirling engines, the second order models offer a good compromise between accuracy, ease of implementation and computational cost.

These models require accurate heat transfer models which have the largest effect on the engine performance. Bergman et al. [8] studied the performance of single acting Stirling engines using the three control volumes approach. They took the instantaneous in cylinder heat transfer for a plain cylinder and the instantaneous regenerator temperature into account. For an over-squared Stirling engine with stroke to bore ratio of *1/10*, they pointed out that the total heat transfer can be enhanced using isothermalizer or fins which increase the heat transfer area. Campos et al. [21] used the finite time heat transfer model with three control volumes on a proposed two cylinder Stirling engine, in which the two cylinders are part of a four cylinder Siemens configuration. This model considered the transfer of thermal energy through tubular heat exchangers only.

The isothermal model which is employed in many studies overestimates the performance of real engines by more than 200% [2]. In Stirling engines running at *15Hz* or more, the processes are more nearly adiabatic in both the expansion and compression cylinders [7][22]. However, the adiabatic processes require the use of heat exchangers, in which the expansion and compression are adiabatic processes whilst the heater and cooler are isothermal processes. Indeed, neither the cylinder walls nor the heat exchangers have unlimited heat transfer [1]. So neither the expansion and compression nor the heating and cooling processes can be isothermal. Recently, a new model called comprehensive Polytropic Model of Stirling engine (CPMS) was able to predict the GPU-3 stirling engine power and efficiency with error percentages +1.13% and 0.45% respectively. This acurate result is obtained by including the polytropic heat transfer in the heater and cooler [23]. This model is based on previous models by the same authers that consider both the expansion and compression as polytropic processes and take into account the heat transfer in these processes [24][25].

In this contribution, a novel non-tubular Franchot engine which is only heated using the cylinder walls and is shown in Figure 2, is studied mathematically with the aim of improving the efficiency and power density of medium temperature Stirling engines. The heat transfer rate is improved due to the large cylinder area, large Reynolds number, low hydraulic diameter and most importantly, the high temperature difference between the cylinder walls and the bulk gas temperatures. Since the Franchot engine has no shuttle or axial conduction losses, the under square engine configuration is adopted with large stroke/bore ratio. This will increase the total surface area and reduce the hydraulic diameter. The mathematical model is used to evaluate the effect of changing the phase angle, engine speed, dead volume, piston diameter and mass charge of an air filled Franchot engine on output power and efficiency.

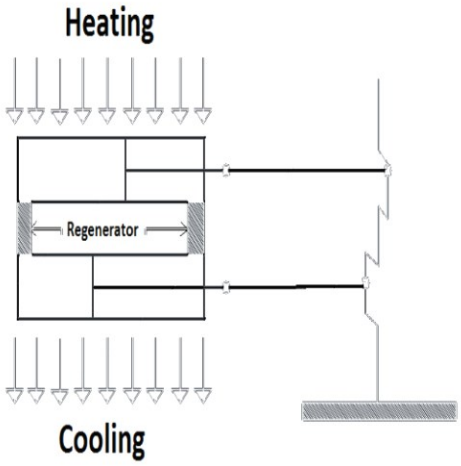

Figure 2: The proposed non-tubular Franchot engine.

2. Mathematical modelling

The polytropic expansion and compression for each half Franchot engine is modelled using a second order model and the three control volumes approach. A schematic of this model is shown in Figure 3. The model is developed in Matlab/Simulink and takes into account the instantaneous heat transfer. On the other hand, shuttle and axial heat losses don't exist in the Franchot engine. Also, in this novel design the effect of the gas spring is less important due to the large temperature difference between the gas and the heat exchanger walls. The heat exchanger gas friction is small due to using a compact design and less material due to elimination of the heater and cooler. This model is limited to the actual Stirling engine and doesn't include the mechanical connection. In this study the cylinder walls are kept at constant and uniform temperatures of *600K* and *300K* for the expansion and compression cylinders, respectively.

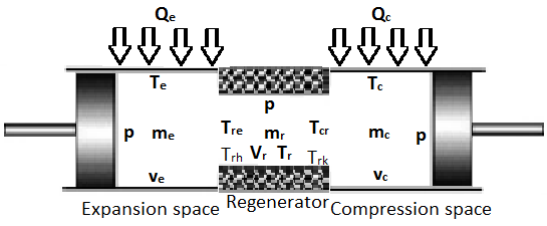

Figure 3: Schematic model of three control volume Stirling engine showing the expansion space, the regenerator and the cooler.

2.1 Ideal model assumptions

In this contribution the ideal behaviour of the non-tubular Franchot engine with polytropic expansion/compression is investigated. Thus the mathematical model describes the ideal system through the following assumptions:

- The engine can be modelled as three compartments: compression, expansion and regenerator.
- Each compartment has uniform instantaneous temperature, pressure and mass.
- Mass is preserved and the total amount is constant.
- No pressure drop occurs.
- No fluid leakage occurs across the power pistons.
- The ideal gas law applies.
- The engine speed is constant and the variation of swept volumes is described by sinusoidal waves.
- Steady state of the cycle occurs.
- Kinetic energy of the working fluid is neglected.
- The regenerator is ideal.
- The cylinder wall temperatures are constant and uniform. This is due to high thermal conductivity of metals in comparison to gases as well as the uniform supply of energy to the external cylinder walls.
- No mechanical losses occur.

These assumptions lead to a model which describes the ideal Stirling engine with limited heat transfer and can be used to analyse the upper performance limits. In subsequent contributions a number of these assumptions will be relaxed to arrive at a more realistic model. In particular, the losses in the regenerator, pressure drop and gas leakage as well as the mechanical connection between the cylinders will be investigated in a future contribution.

2.2 Thermodynamic modelling

The Stirling engine is modelled through mass and energy balances in the three control volumes which are connected through mass and energy flow across the volume boundaries.

The mass balance of the three control volumes is given by

$$M = m_e + m_c + m_r \quad (1)$$

where $\boldsymbol{M, m_e, m_c \text{ and } m_r}$ are the total constant gas mass inside the engine, the expansion volume gas mass, the compression volume gas mass and the trapped regenerator gas mass. Due to the constant total gas mass, the derivative of Equation 1 is given by

$$0 = \dot{m}_e + \dot{m}_c + \dot{m}_r \quad (2)$$

By assuming that the working gas is an ideal gas, the equation of state for the three control volumes can be written as

$$pv_x = m_x R\, T_x \quad (3)$$

where $\boldsymbol{p}$ is the instantaneous pressure, $\boldsymbol{v_x}$ is the control volume, $\boldsymbol{m_x}$ is the control volume gas mass, R is the ideal gas constant and $\boldsymbol{T_x}$ is the control volume gas temperature.

The energy balance equation for the expansion space is given by

$$\dot{Q}_e + c_p \dot{m}_e T_{re} = p\dot{v}_e + c_v(\dot{m_e T_e}) \quad (4)$$

Rearranging Equation 4 for the change in expansion volume gas mass, i.e. mass flow rate in the expansion cylinder, results in

$$\dot{m}_e = \frac{\frac{p\dot{v}_e}{R} + \frac{v_e \dot{p}}{\gamma R} - \frac{\dot{Q}_e}{c_p}}{T_{re}} \quad (5)$$

Similarly, the compression cylinder mass flow rate is given by

$$\dot{m}_c = \frac{\frac{p\dot{v}_c}{R} + \frac{v_c \dot{p}}{\gamma R} - \frac{\dot{Q}_c}{c_p}}{T_{cr}} \quad (6)$$

Using the ideal gas law and assuming that the regenerator average temperature is constant the regenerator mass flow rate is calculated as

$$\dot{m}_r = \frac{V_r}{RT_r}\dot{p} \quad (7)$$

By combining Equations 2, 5, 6 and 7 the differential form of the pressure is obtained

$$\dot{p} = \frac{-p\left(\frac{\dot{v}_e}{T_{re}} + \frac{\dot{v}_c}{T_{cr}}\right) + \frac{R}{c_p}\left(\frac{\dot{Q}_e}{T_{re}} + \frac{\dot{Q}_c}{T_{cr}}\right)}{\frac{v_e}{\gamma T_{re}} + \frac{V_r}{T_r} + \frac{v_c}{\gamma T_{cr}}} \quad (8)$$

where T_{re} and T_{cr} are the temperatures of the gas entering and leaving the hot regenerator end and of the gas entering and leaving the cold regenerator end, respectively. These temperatures are calculated through

$$T_{re} = \begin{cases} T_e, & \dot{m}_e < 0 \\ T_{rh}, & \dot{m}_e \geq 0 \end{cases} \quad (9)$$

$$T_{cr} = \begin{cases} T_c, & \dot{m}_c < 0 \\ T_{rk}, & \dot{m}_c \geq 0 \end{cases} \quad (10)$$

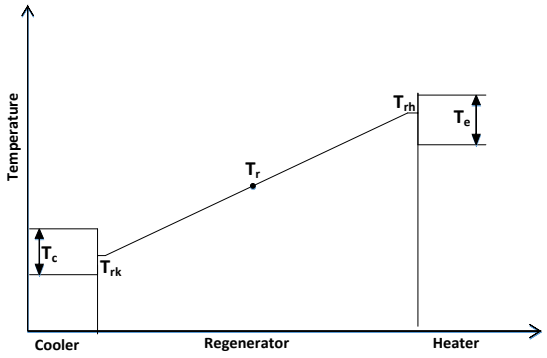

Figure 4: Ideal temperature performance of the 3 control volume Stirling engine.

The regenerator temperature is shown in Figure 4 and defined as

$$T_r = \frac{T_{rh} - T_{rk}}{\ln\frac{T_{rh}}{T_{rk}}} \quad (11)$$

where T_{rh} and T_{rk} are the regenerator hot and cold end temperatures, considered as constant temperatures and found from the regenerator energy balance equation

$$\dot{Q}_r + c_p \dot{m}_e T_{re} + c_p \dot{m}_c T_{cr} = \frac{c_v}{R} V_r \dot{p} \quad (12)$$

Taking the closed integration of Equation 12 over one cycle results in

$$\oint c_p \dot{m}_e T_{re} + \oint c_p \dot{m}_c T_{cr} = 0 \quad (13)$$

By assuming ideal regeneration, the energy from the hot regenerator side doesn't transfer to the cold side and thus for the hot side only the first integral needs to be considered. This integral can be rearranged to

$$\oint [ic_p \dot{m}_e T_e + (1-i)c_p \dot{m}_e T_{rh}] = 0 \qquad (14)$$

which gives the following equation for T_{rh}

$$T_{rh} = \frac{-\oint i\dot{m}_e T_e}{\oint (1-i)\dot{m}_e} \qquad (15)$$

Similarly, the temperature of the cold side is given by

$$T_{rk} = \frac{-\oint j\dot{m}_c T_c}{\oint (1-j)\dot{m}_c} \qquad (16)$$

In equations 14-16 the parameters i and j are given by

$$i = \begin{cases} 1, & \dot{m}_e < 0 \\ 0, & \dot{m}_e \geq 0 \end{cases} \qquad (17)$$

$$j = \begin{cases} 1, & \dot{m}_c < 0 \\ 0, & \dot{m}_c \geq 0 \end{cases} \qquad (18)$$

The mass flow rate $\dot{m}_e$ is calculated from Equation 5 while $\dot{m}_c$ and m_c are calculated from Equations 2 and 1, respectively.

Once the mass and energy flows are calculated the output power is evaluated as

$$P_{ins} = \Delta p(\dot{v}_e + \dot{v}_c) \qquad (19)$$

where P_{ins} and Δp are the mechanical instantaneous power and the instantaneous pressure difference across pistons. The cycle work is calculated as

$$w = \oint \Delta p(\dot{v}_e + \dot{v}_c) \qquad (20)$$

thus the average power can be written as

$$P = \oint \Delta p(\dot{v}_e + \dot{v}_c) * f \qquad (21)$$

2.3 Heat transfer

The cylinder heat transfer of a Stirling engine can be described by Newton's law of cooling, describing convective heat transfer. The head added to the expansion cylinder is given by

$$\dot{Q}_e = hA_e(T_h - T_e) \qquad (22)$$

and the rejected heat by the compression cylinder is given by

$$\dot{Q}_c = hA_c(T_k - T_c) \qquad (23)$$

Here $\boldsymbol{h}, \boldsymbol{A_e}, \boldsymbol{A_c}, \boldsymbol{T_h}$ and $\boldsymbol{T_k}$ are the heat transfer coefficient, instantaneous expansion cylinder wall area, instantaneous compression cylinder wall area, expansion cylinder wall temperature and compression cylinder wall temperature, respectively.

Most researchers used constant heat transfer rates in Equations 22 and 23. For example, Martaj et al. [26] used an isothermal model to study a low temperature differential Stirling engine with limited heat transfer. The heat is added through a flat plate and not the cylinder wall so neither the convective heat transfer coefficient, gas temperature nor conducting area were variable.

Some publications consider an instantaneous convective heat transfer coefficient. For example [27][19] used non-dimensional correlations to describe the natural convective heat transfer in Stirling engines, while Shazly et al. [28] used equations based on Nusselt, Grasshof and Prandtl numbers to calculate the natural heat convection for a direct solar powered Stirling engine. A number of other contributions used correlations based on forced convective heat transfer [8][21][20]. Most of these correlations were originally developed for internal combustion engines or compressors [29][30][31]. Stirling engines differ from these due to the absence of valves and thus the swirl gas velocity inside Stirling engines is higher [8][32]. In this study the under-squared engine has a large stroke to bore ratio and high Reynolds number unlike internal combustion engines or compressors, so requires a tailored correlation.

Stirling engine heat transfer rates can be modelled using the Nusselt number pipe model aRe^b [29]. However, Toda et al. [32] showed that the instantaneous heat transfer for Stirling engines is not accurately described by the pipe model, namely $Nu = 0.023Re^{0.8}$.

Instead, they obtained two correlations tailored to Stirling engines: Equation 24 correlates the Nusselt number with the instantaneous Reynolds number for Stirling engines.

$$Nu = \begin{cases} 0.7Re^{0.58}\ expantion\ stroke \\ 0.62Re^{0.53}\ compression\ stroke \end{cases} \quad (24)$$

where

$$Nu = \frac{hD_x}{k} \quad (25)$$

and Equation 26 directly correlates the instantaneous heat transfer coefficient with the piston diameter, flow velocity, pressure and temperature.

$$h_e = 0.042D^{-0.42}v^{0.58}p^{0.58}T^{-0.19}$$
$$h_c = 0.0236D^{-0.47}v^{0.53}p^{0.53}T^{-0.11} \quad (26)$$

These correlations were developed for air filled engines working at temperatures ranges from room temperature up to 400°C. Thus in this study Equation 26 is used as it was developed for medium temperature, air charged Stirling engines.

3 Numerical results and discussion

The mathematical model from Section 2 is implemented in Matlab/Simulink and used to analyse the performance of small scale engines at moderate temperatures, i.e. up to 600K. The parameters of the reference non-tubular Franchot engine design are shown in Table 1. This configuration is called the reference engine design and used for most simulations unless otherwise mentioned.

The maximum stroke of the Stirling engine is chosen to be 25cm because larger strokes are difficult to implement: the length of the connecting rod needs to be at least double the stroke length and the crank radius needs to be half of the stroke length which would make the system larger and bulkier. Instead of changing the stroke length, the diameter of the cylinder is changed to evaluate changes in the stroke to bore ratio. In addition, the phase angle, engine speed, dead volume and charge densities are changed to evaluate their effect on the performance. The hot cylinder wall temperature was keep constant at 600K due to thermal limitations of the hot piston seal and correlates with the temperature range of one axis solar parabolic collectors.

Table 1: Parameters of the reference engine

Name	symbol	value/unit
Stroke length	L_e, L_c	*25cm*
Bore diameter	D_e, D_c	*2cm*
charge gas density	ρ	*1.225kg/m³*
Charge pressure		*1atm*
Clearance length	re, rc	*1mm*
Regenerator volume	V_r	*0cm³*
Swept volume ratio		*1*
Dead volume ratio		*1*
Out of Phase angle	θ	*150 deg*
Engine speed	n	*1000RPM*
Hot cylinder temperature	T_h	*600K*
Cold cylinder temperature	T_k	*300K*
Working gas		*Air*
Gas constant	R	*287J/kg.K*

3.1 Effect of changing the phase angle

The phase angle is the thermodynamic lag angle for the compression to the expansion spaces. The effect of changing the phase angle on the efficiency and power for the reference engine design is shown in Figure 5. It can be seen, that phase angles between 150°-170° have simultaneously high efficiency and high power and are thus the most suitable phase angles for the ideal reference design. The performance in this phase angle range can be optimised between the highest power and the highest efficiency.

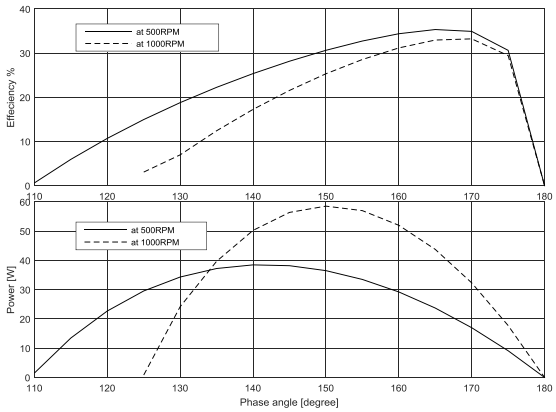

Figure 5: Variation of engine output efficiency and power with phase angle for the reference engine at 500 and 1000 RPM

However, the maximal power phase angle (150^o) and maximal efficiency phase angle (170^o) are distinct for the reference engine, so that the engine cannot be optimised for both performance criteria simultaneously. While in this configuration the difference is only 20^o, the difference in the efficiency and power at those phase angles is significant: 25.3% efficiency and 58.5W at 150^o and 33% efficiency and 32.3W at 170^o. The efficiency 25.3% at the maximum power shows a good match with the ideal efficiency of 29.3% calculated by Curzon and Ahlborn [18]. The small reduction in efficiency is most likely due to the non-isothermal expansion and compression. This shows that the Curzon and Ahlborn efficiency cannot be achieved even with an ideal engine unless the heat transfer is infinite. At lower speeds the engine achieves less power but with better efficiencies. This is due to the decrease in the indicated power in comparison to the heat transfer. In addition, at lower speeds the optimum phase angles are shifted towards smaller angles.

Stirling engines are usually designed to work at the highest power speeds, in order to increase the power densities and hence reduce the capital cost. In the non-tubular Franchot engine, the power and efficiency can be improved by changing the phase angle without increasing the engine complexity. In Figure 6 the PV diagram of a half Franchot engine which is a conventional alfa type engine shows that increasing the phase angle decreases the maximum engine pressure and decreases the added and rejected thermal energies. This reduces the internal heating and cooling loads on the heating and cooling cylinders as well as the gas leakage.

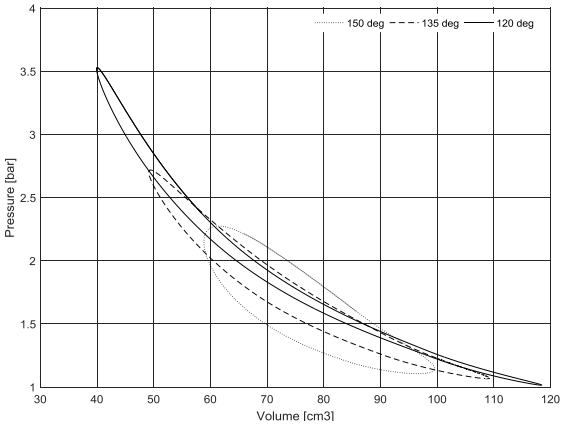

Figure 6: P-V (work) diagram of the reference engine at different phase angles

The instantaneous gas temperatures inside both the expansion and compression volumes can be seen in Figure 7. The temperature difference between the cylinders walls and the bulk gas temperatures is large. Hence a possibility for gas spring loss is slim.

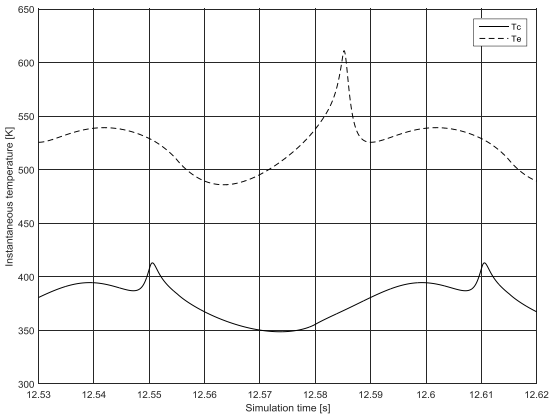

Figure 7: The bulk gas temperatures of the basic engine design

The relationship between phase angle and engine speed is illustrated in Figure 8. It can be seen that the engine output power increases at higher speeds for increasing phase angles and that the efficiency decreases with increasing engine speed. For each engine speed there is one phase angle which gives the highest power but not the highest efficiency. The maximum power efficiency, i.e. the efficiency at the

maximum output power, is around 17% for all studied phase angles.

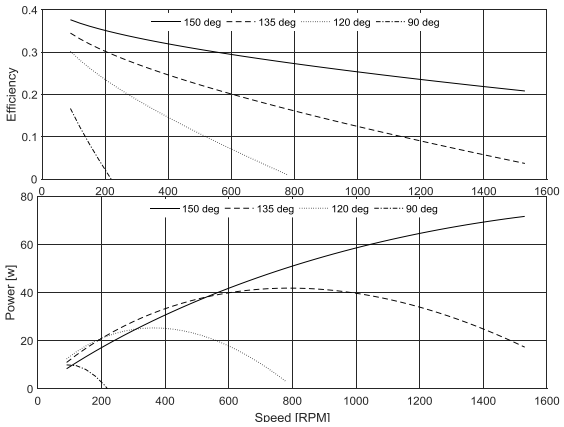

Figure 8: Variation of engine efficiency and power with engine speed at various phase angles.

Generally, increasing the speed leads to a linear increase in the indicated power which is given by equation 21, while the heat transfer given by equation 26 increases with a slower rate.

This engine is a special case that has zero dead volume. However, the dead volume can lead to a decrease in the power density which will be investigated in the next section.

3.2 Effect of the dead volume

The dead volume ratio is the ratio of the clearance volume to the swept volume. So far, the simulations were performed with a dead volume ratio of 25%, 50%, 100% and 200% of the swept volume. It is assumed that the dead volume is at the head of the cylinder so an increase in the dead volume goes along with an increase of the cylinder wall area which acts as the heat transfer area. Thus an increase in the dead volume increases the energy transfer into and out of the cylinder. However, the dead volume also decreases the indicated power by decreasing the pressures.

Figure 9 shows that for a fixed phase angle of 90^o, an increase in the dead volume improves the efficiency and increases the maximum power at higher speeds. The increase in dead volume has a similar effect than an increase in phase angle. However, at each single speed neither the maximum power nor its efficiency was found to be better than that achieved by tuning the phase angle. Thus it would be beneficial to increase the number of power pistons at the optimal phase angle instead of increasing the dead volume to achieve higher engine powers. For example, doubling the engine size by increasing the dead volume doesn't double the maximum engine power at the same speed.

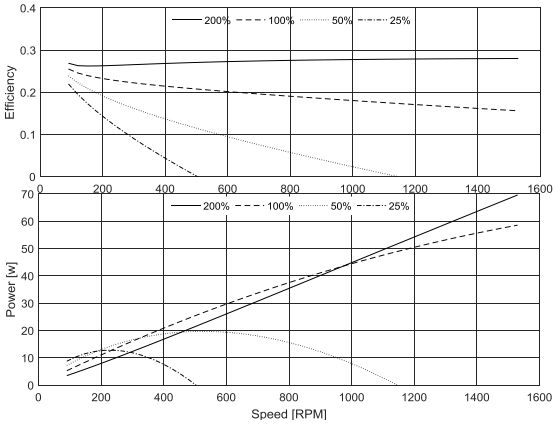

Figure 9: Variation of engine efficiency and power with engine speed at various dead volume ratios at 90^{o}phase angle.

3.3 Effect of the cylinder diameter

Figure 10 shows the response of the non-tubular Franchot engine to changing the piston diameter while keeping the stroke length constant. The heat transfer correlations in Equation 26 remain valid for these stroke to bore ratios. It can be seen that smaller diameters always increase the efficiency but not necessarily the power at a fixed phase angle because the swept volume is smaller. The higher efficiency results from higher heat transfer coefficients which are due to higher Reynolds numbers and smaller hydraulic diameters. Smaller diameters have a decreased swept volume, hence a decreased indicated power. The rate of decreasing the swept volume is larger than the decrease in the heat transfer.

At low speeds and a fixed phase angle larger diameter pistons give higher power because the heat transfer is fast enough to deliver the required energy. However, small piston

diameters are not able to compete at low speeds unless the phase angle is reduced to force the engine to work at a higher power mode. In addition, decreasing the diameter can increase the pumping losses in real engines which inhibits the engine from working at higher speeds. The maximum power efficiency is around 16.5% for the studied diameters.

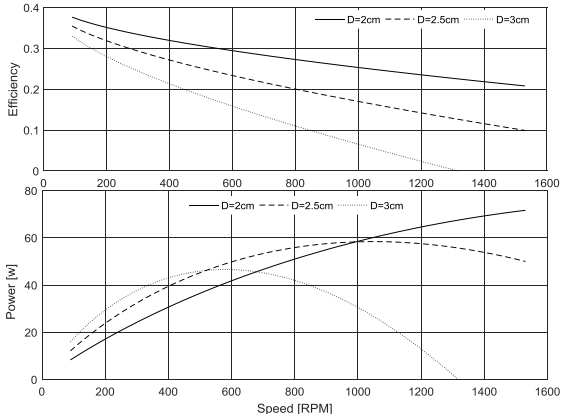

Figure 10: Variation of engine output efficiency and power with engine speed at various piston diameters.

3.4 Effect of the charge density

The effect of the charge air density is shown in Figure 11. Although the effect on the maximum power is barely noticeable, it decreases the corresponding maximum power speed. In addition, the maximum power efficiency is around 16.5% for all studied densities. This result makes pressurising the working gas unavoidable if higher power is needed and higher speeds are unreachable. However, an increase in charge density increases the requirements on the engine sealing. In this case it might be advantageous to replace air with Helium which has a better capability factor that leads to higher heat transfers, higher speed ranges and reduced losses.

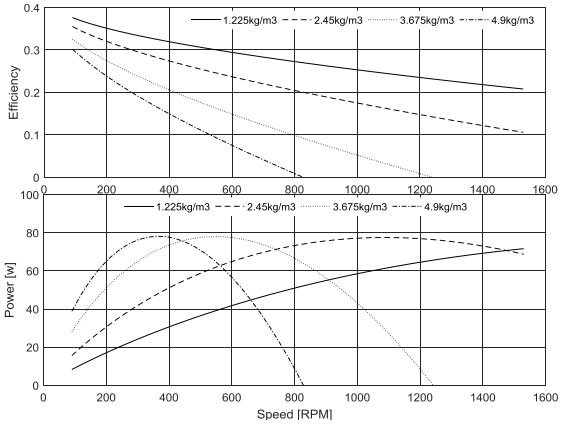

Figure 11: Variation of engine output efficiency and power with engine speed at various charge densities

Figure 12 shows the decrease of both the pressure and pressure difference peaks on the working pistons for increasing phase angles for two charge densities. The lower pressure differences at larger phase angles result in decreasing gas leakage losses across the power pistons. Figure 12 also shows a steep decrease of the pressure and pressure difference peaks for the pressurised engine at 2.45kg/m^3. The decrease in the maximum pressure results in lower requirements on the engine material and mass and also decreases the leakage of the working gas to the ambient through the connecting rod sleeves.

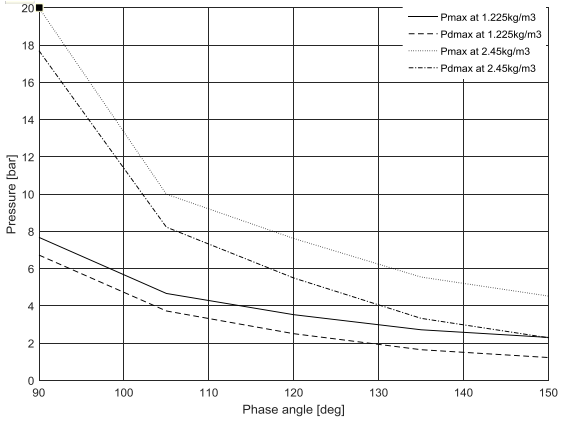

Figure 12: Variation of engine max pressure and piston pressure difference with phase angle at two charge densities.

4 Conclusion

The variations of performance of the novel non-tubular Franchot engine due to changing the engine speed, phase angle, dead volume, piston diameter and air charge density were investigated.

The thermodynamic model developed for the Franchot Stirling engine is based on the three control volume approach with polytropic expansion and compression and limited instantaneous heat transfer. The heat transfer during a cycle is not constant due to the variations of working gas temperature, side wall area and the convective heat transfer coefficient. This polytropic model is capable of more accurate predictions of the Stirling engine performance compared to the widely used isothermal and adiabatic models. The model was implemented in Matlab/Simulink and shows good agreement between the maximum power efficiency and the ideal efficiency calculated by Curzon and Ahlborn.

It is shown that the phase angle has a large effect on the engine performance. By increasing the phase angle from 90^o (the fixed phase angle for the 4 cylinder Siemens engine) the engine output power as well as the efficiency is increased up to a maximum at a phase angle of 150^o and 170^o, respectively. In addition, the pressure difference across the power piston is reduced to less than 25% which leads to a significant reduction in gas leakage which was identified as one of the main drawbacks of the Franchot compared to the Siemens engine. Changing the phase angle doesn't affect any of the physical components or the gas density, but simply shifts the maximum power to higher speeds. Thus operating the Franchot engine at higher phase angles removes one of the main disadvantages compared to the Siemens engine and thus the Franchot engine could be better at low to medium temperatures.

In addition, it was shown that increasing the air charge density, the maximum power point is shifted to lower speeds without causing any significant change in the efficiency or power. This is important because in real engines the losses as well as the heat transfer rates determine the maximum engine speed.

Thus the results of this study show that it is possible to increase both engine power and efficiency at lower speeds by optimising both the phase angle and working gas density. In conclusion, if freed from the operational constraints of the Siemens engine, the Franchot engine has the potential to be superior to the Siemens engine.

Acknowledgement

The authors would like to thank HESPAL for the PhD scholarship for Jafar Daoud.

References

[1] D. G. Thombare and S. K. Verma, "Technological development in the Stirling cycle engines," *Renew. Sustain. Energy Rev.*, vol. 12, no. 1, pp. 1–38, Jan. 2008.

[2] A. Sripakagorn and C. Srikam, "Design and performance of a moderate temperature difference Stirling engine," *Renew. Energy*, vol. 36, no. 6, pp. 1728–1733, Jun. 2011.

[3] a. Asnaghi, S. M. Ladjevardi, P. Saleh Izadkhast, and a. H. Kashani, "Thermodynamics Performance Analysis of Solar Stirling Engines," *ISRN Renew. Energy*, vol. 2012, pp. 1–14, 2012.

[4] T. Mancini, P. Heller, B. Butler, B. Osborn, W. Schiel, V. Goldberg, R. Buck, R. Diver, C. Andraka, and J. Moreno, "Dish-Stirling Systems: An Overview of Development and Status," *J. Sol. Energy Eng.*, vol. 125, no. 2, p. 135, 2003.

[5] F. Alberti and L. Crema, "Design of a new medium-temperature Stirling engine for distributed cogeneration applications," *Energy Procedia*, vol. 57, pp. 321–330, 2014.

[6] B. Kongtragool and S. Wongwises, "Performance of low-temperature differential Stirling engines," *Renew. Energy*, vol. 32, no. 4, pp. 547–566, 2007.

[7] G. Walker, *Cryocoolers*, Part 2: Ap. Boston, MA: Springer US, 1983.

[8] C. Bergmann, A. N. D. J. Albert, and D. O. S. Reis, "NUMERICAL PREDICTION OF THE INSTANTANEOUS REGENERATOR AND IN-CYLINDER HEAT TRANSFER OF A STIRLING ENGINE," *Int. J. ENERGY Res.*, vol. 15, no. November 1990, pp. 623–635, 1991.

[9] G. Walker, "Coal-fired Stirling engines for

railway locomotive and stationary power applications," *Proc lnstn Mech Engrs*, vol. 197A, no. October, pp. 233–246, 1983.

[10] B. Hoegel, D. Pons, M. Gschwendtner, and A. Tucker, "Theoretical investigation of the performance of an Alpha Stirling engine for low temperature applications," *ISEC Int. Stirling Engine Comm.*, no. January, 2012.

[11] B. Hoegel, "Thermodynamics-based design of stirling engines for low-temperature heat sources.," University of Canterbury, 2014.

[12] B. Hoegel, D. Pons, M. Gschwendtner, A. Tucker, and M. Sellier, "Thermodynamic peculiarities of alpha-type Stirling engines for low-temperature difference power generation: Optimisation of operating parameters and heat exchangers using a third-order model," *Proc. Inst. Mech. Eng. Part C J. Mech. Eng. Sci.*, vol. 228, no. 11, pp. 1936–1947, 2014.

[13] W. . Arias, H. I. . Velásquez, D. . Florez, and S. . Oliveira Junior, "Thermodynamic analysis, performance numerical simulation and losses analysis of a low cost Stirling engine V-Type, and its impact on soc Efficiency, Cost, Optimization, Simulation and Environmental Impact of Energy Systems, ECOS 2011ial development in rem," *Proc. 24th Int. Conf.*, pp. 3767–3778, 2011.

[14] J. R. Senft, "Optimum Stirling engine geometry," *Int. J. Energy Res.*, vol. 26, no. 12, pp. 1087–1101, 2002.

[15] N. Martaj and P. Rochelle, "1D modelling of an alpha type Stirling engine," *Int. J. Simul. Multidiscip. Des. Optim.*, vol. 5, p. A07, 2014.

[16] B. Kongtragool and S. Wongwises, "A review of solar-powered Stirling engines and low temperature differential Stirling engines," *Renew. Sustain. Energy Rev.*, vol. 7, no. 2, pp. 131–154, 2003.

[17] J. D. Van de Ven, "Mobile hydraulic power supply: Liquid piston Stirling engine pump," *Renew. Energy*, vol. 34, no. 11, pp. 2317–2322, 2009.

[18] F. L. Curzon and B. Ahlborn, "Efficiency of a Carnot engine at maximum power output," *Am. J. Phys.*, vol. 43, no. 1, pp. 22–24, Jan. 1975.

[19] K. KRAITONG, "NUMERICAL MODELLING AND DESIGN OPTIMISATION OF STIRLING ENGINES FOR POWER PRODUCTION," University of Northumbria at Newcastle, 2012.

[20] M. Babaelahi and H. Sayyaadi, "Modified PSVL: A second order model for thermal simulation of Stirling engines based on convective-polytropic heat transfer of working spaces," *Appl. Therm. Eng.*, vol. 85, pp. 340–355, 2015.

[21] M. C. Campos, J. V. C. Vargas, and J. C. Ordonez, "Thermodynamic optimization of a Stirling engine," *Energy*, vol. 44, no. 1, pp. 902–910, 2012.

[22] G. Walker and J. R. Senft, *Free Piston Stirling Engines*, First edit., vol. 12. Berlin, Heidelberg: Springer Berlin Heidelberg, 1985.

[23] M. Babaelahi and H. Sayyaadi, "Analytical closed-form model for predicting the power and efficiency of Stirling engines based on a comprehensive numerical model and the genetic programming," *Energy*, vol. 98, pp. 324–339, Mar. 2016.

[24] M. Babaelahi and H. Sayyaadi, "A new thermal model based on polytropic numerical simulation of Stirling engines," *Appl. Energy*, vol. 141, pp. 143–159, 2015.

[25] Y. Timoumi, I. Tlili, and S. Ben Nasrallah, "Design and performance optimization of GPU-3 Stirling engines," *Energy*, vol. 33, no. 7, pp. 1100–1114, Jul. 2008.

[26] N. MARTAJ, L. GROSU, and P. ROCHELLE, "Thermodynamic study of a low temperature differences Stirling engine at steady state operation," *Int. J. Appl. Thermodyn.*, vol. 10, no. 4, pp. 165–176, 2007.

[27] N. A.-K. M. Tarawneh, F. Al-Ghathian, M. A. Nawafleh, "Numerical Simulation and Performance Evaluation of Stirling Engine Cycle," *Jordan J. Mech. Ind. Eng.*, vol. 4, pp. 615–628, 2010.

[28] J. H. Shazly, A. Z. Hafez, E. T. El Shenawy, and M. B. Eteiba, "Simulation, design and thermal analysis of a solar Stirling engine using MATLAB," *Energy Convers. Manag.*, vol. 79, pp. 626–639, Mar. 2014.

[29] A. A. Kornhauser, B. C. Kafka, D. L.

Finkbeiner, and F. C. Cantelmi, “Heat Transfer Measurements for Stirling Machine Cylinders,” 1994.

[30] R. P. Adair, E. B. Qvale, and J. T. Pearson, “Instantaneous heat transfer to cylinder wall in reciprocating compressors,” *Int. Compress. Eng. Conf.*, pp. 521–526, 1972.

[31] C. A. Finol and K. Robinson, “Thermal modelling of modern engines: a review of empirical correlations to estimate the in-cylinder heat transfer coefficient,” *Proc. Inst. Mech. Eng. Part D J. Automob. Eng.*, vol. 220, no. 12, pp. 1765–1781, Jan. 2006.

[32] F. Toda, M. Matsuo, and Y. Umezane, “Heat Transfer on a Small Stirling Engine -Heat Transfer in Expansion Chamber Wall - *,” *Bull. M.E.S.J*, vol. 19, no. 1, pp. 49–59, 1991.